Vesicles Formed in Aqueous Mixtures of Cholesterol and Imidazolium Surface Active Ionic Liquid: A Comparison with Common Cationic Surfactant by Water Dynamics

ARTICLE *in* THE JOURNAL OF PHYSICAL CHEMISTRY B · MAY 2014

Impact Factor: 3.3 · DOI: 10.1021/jp501033n · Source: PubMed

7 AUTHORS, INCLUDING:

Sarthak Mandal
Columbia University
44 PUBLICATIONS **444** CITATIONS
SEE PROFILE

Surajit Ghosh
IIT Kharagpur
45 PUBLICATIONS **381** CITATIONS
SEE PROFILE

Chiranjib Banerjee
Aarhus University
35 PUBLICATIONS **236** CITATIONS
SEE PROFILE

Nilmoni Sarkar
IIT Kharagpur
159 PUBLICATIONS **3,691** CITATIONS
SEE PROFILE

THE JOURNAL OF PHYSICAL CHEMISTRY B

Article

pubs.acs.org/JPCB

Vesicles Formed in Aqueous Mixtures of Cholesterol and Imidazolium Surface Active Ionic Liquid: A Comparison with Common Cationic Surfactant by Water Dynamics

Sarthak Mandal, Jagannath Kuchlyan, Surajit Ghosh, Chiranjib Banerjee, Niloy Kundu, Debasis Banik, and Nilmoni Sarkar*

Department of Chemistry, Indian Institute of Technology, Kharagpur 721302, WB, India

Supporting Information

ABSTRACT: The formation of stable unilamellar vesicles which hold great potential for biological as well as biomedical applications has been reported in the aqueous mixed solution of a surface active ionic liquid (SAIL), 1-hexadecyl-3-methylimidazolium chloride ([C_{16}mim]Cl) and cholesterol. To make a comparison we have also shown the formation of such stable vesicles using a common cationic surfactant, benzyldimethylhexadecylammonium chloride (BHDC) which has a similar alkyl chain length but different headgroup region to that of [C_{16}mim]Cl. It has been revealed from dynamic light scattering (DLS), transmission electron microscopy (TEM), nuclear magnetic resonance (NMR), and other optical spectroscopic techniques that the micelles of [C_{16}mim]Cl and BHDC in aqueous solutions transform into stable unilamellar vesicles upon increasing concentration of cholesterol. We find that, as the concentration of cholesterol increases, the solvation and rotational relaxation time of C153 in [C_{16}mim]Cl/cholesterol solution as well as in BHDC/cholesterol solution gradually increases indicating a significant decrease in the hydration behavior around the self-assemblies upon micelle−vesicle transition. However, the extent of increase in solvation and rotational relaxation time is more prominent in the case of [C_{16}mim]Cl/cholesterol solutions than in the BHDC/cholesterol system. This indicates that [C_{16}mim]Cl/cholesterol vesicular membranes are comparatively less hydrated and more rigid than the BHDC/cholesterol vesicular bilayer.

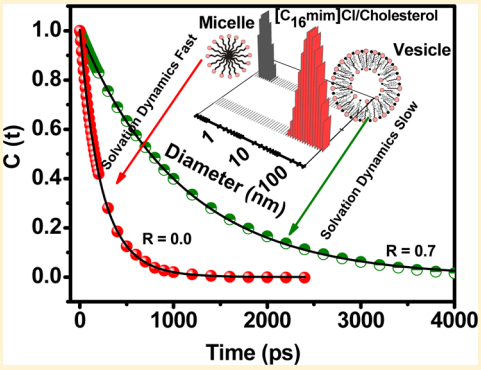

INTRODUCTION

Over the past few decades, liposomes composed of phospholipids have been extensively studied as drug and gene delivery systems because of their unique ability to solubilize both the hydrophobic and hydrophilic molecules.[1−4] It has been well reported that liposomes can enhance the drug stability, therapeutic effects, and uptake of the solubilized drug into the target site with reduced toxicity. However, the stability of liposomes is limited by the hydrolytic and oxidative degradation of phospholipids. Moreover, because of the poor aqueous solubility of the phospholipids, the stability of their vesicular structures is also kinetically limited as they are prone to form a collapsed planar lamellar structure which is the equilibrium state of aggregation.[5] The lack of physical and chemical stability of the liposomes restricts their usage as drug carriers and models for biological membranes. Therefore, the search for new supramolecular vesicles of alternative substances is a long-standing topic of research. The past few years have witnessed a significant drug delivery shift in the biomedical arena by developing various new nonphospholipid vesicular systems composed of common surfactants and polymers.[6−13]

In recent years, surface active ionic liquids (SAILs) capable of forming various self-assembled nanostructures have earned significant interest in the field of chemistry and biology.[14−20] SAILs are basically referred to as the long alkyl chain containing ionic liquids which exhibit surface active properties.[21−23] SAILs have recently emerged as a novel class of surfactants because of the unique properties of RTILs. Extensive studies have been performed on the self-assembly behavior of SAILs in aqueous and nonaqueous media.[24−30] Numerous recent studies have indicated that SAILs, particularly imidazolium-based SAILs, exhibit greater surface activity than conventional surfactants in aqueous and nonaqueous media.[25] This provides the primary impetus to formulate more advanced self-assembled nanostructures of SAILs (such as versicles) which can be used as a possible drug delivery medium. There are only a few reports on the vesicular properties of SAILs in aqueous solutions. In a recent study, Wang et al.[27] demonstrated the microstructural transition of spherical micelles to unilamellar vesicles with the increase in concentration of 1-alkyl-3-methylimidazolium bromides [$C_n$mim]Br (n = 10, 12, 14) in aqueous solutions without any additives. It is also known that these long alkyl chain containing SAILs aggregate into a vesicular structure in

Received: January 29, 2014
Revised: April 5, 2014
Published: May 8, 2014

the presence of external additives such as common surfactants or aromatic molecules.[28,29]

In this paper, we have demonstrated the formation of stable unilamellar vesicles composed of cholesterol and an imidazolium-based SAIL, [C_{16}mim]Cl. To make a comparison of the vesicular properties of SAIL with those of a structurally related common cationic surfactant, we have also shown the formation of vesicles in the aqueous mixture of cholesterol and surfactant BHDC. The formation of vesicles in the mixture of cholesterol with other common cationic and nonionic surfactants has been well reported in literature to be similar to the micelle-vesicle transitions in the mixture of cationic and anionic surfactants systems.[31−40] Both [C_{16}mim]Cl and BHDC are well reported to form micelles in the aqueous solution above their critical micelle concentrations (CMCs).[26,41] It has been established that the superior surface activity and directional polarizability of SAILs help prepare highly ordered self-assemblies that can exhibit very different or even improved templating behavior in the synthesis of nanomaterials.[30] Another basic advantage of using SAILs in the formation of vesicles is that their cationic and anionic constituents can easily be tuned according to the desired properties. Therefore, the study of SAILs on the formation of novel supramolecular vesicles is fruitful and intriguing. The aim of this present work is to establish the difference between [C_{16}mim]Cl/cholesterol and BHDC/cholesterol self-assemblies in terms of their hydration behavior and rigidity.

The detailed characterizations of both [C_{16}mim]Cl/cholesterol and BHDC/cholesterol solutions with varying concentration of cholesterol were performed systematically using phase behavior, dynamic light scattering, transmission electron microscopy, NMR, and various other useful optical spectroscopic techniques. The structural and dynamical properties of the vesicles are found to be significantly varied on increasing the cholesterol content. Moreover, the ionic liquid forming self-assemblies are markedly different from the common surfactant assemblies if we compare the structural properties in terms of membrane rigidity and hydration behavior.

It is known that the water molecules present around the hydration layer of the self-assemblies plays an important role in controlling the structure, dynamics, and heterogeneity of the systems.[42−46]These confined water molecules show very different properties with respect to the viscosity, polarity, pH, and mobility from those of bulk water. In many natural and biological systems, the structure, functions, and reactivity are controlled in part by the water present in the interfaces of various biomolecules such as DNA and proteins.[47,48] Since micelles, mixed micelles, and vesicles can mimic many complex biological systems in a much simpler form, the study of water dynamics in the hydration layer of these self-assemblies has gained significant interest in recent years.[49,50] In the present work, we have therefore explored the dynamics of water molecules around the hydration layer of the two newly developed supramolecular assemblies, namely SAIL/cholesterol and BHDC/cholesterol self-assemblies at varying cholesterol content from $R = 0$ to 1. The changes in the hydration behavior in the course of micelles-to-vesicle transitions have been monitored by using sensitive solvation and rotational relaxation dynamics studies where coumarin 153 (C153) has been used as a fluorescent probe. The solvation dynamics within the various nanostructures of proteins, phospholipids, surfactants, and RTILs have been extensively studied in the past few years by various spectroscopic and molecular dynamics simulation methods in order to understand their structural heterogeneity.[51−57] However, to the best of our knowledge, this is the first report which focuses on the dynamics of the supramolecular assemblies composed of cholesterol and an imidazolium SAIL. We found that the hydration behavior of the self-assemblies is remarkably reduced as micelles are gradually transformed into vesicles upon increasing cholesterol content. Moreover, from the solvation and rotational relaxation times of C153 in [C_{16}mim]Cl/cholesterol and BHDC/cholesterol solutions one can easily understand the difference in hydration behavior and membrane rigidity between the SAIL assemblies and common surfactant assemblies. This work also examined the applicability of solvation and the rotational relaxation dynamics method to probe micelle−vesicle transitions.

2. EXPERIMENTAL SECTION

2.1. Materials. 1-Hexadecyl-3-methylimidazolium chloride ([C_{16}mim]Cl) was obtained from Kanto Chemicals (98% purity). Benzyldimethylhexadecylammonium chloride (BHDC) was used as received from Sigma-Aldrich. Cholesterol (99% purity) was purchased from SRL, India. All of the above chemicals were used without further purification. Double distilled Milli-Q water was used for the preparation of solutions. Coumarin 153 (C153, laser grade) was used as received from Exciton. The chemical structures of [C_{16}mim]Cl, BHDC, cholesterol, and C153 are shown in Scheme 1.

Scheme 1. Chemical Structure of [C_{16}mim]Cl, BHDC, Cholesterol, and C153

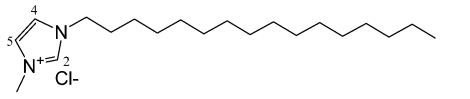

1-Hexadecyl-3-methylimidazolium chloride ([C_{16}mim]Cl)

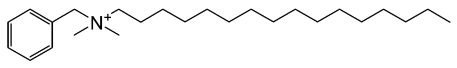

Benzyldimethylhexadecylammonium chloride (BHDC)

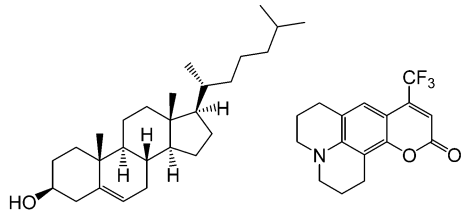

Cholesterol Coumarin 153 (C153)

2.2. Preparation of Solutions. To prepare [C_{16}mim]Cl/cholesterol and BHDC/cholesterol vesicular solutions of varying cholesterol content, first appropriate amounts of [C_{16}mim]Cl and BHDC were taken in separate glass bottles so that the final concentration of [C_{16}mim]Cl and BHDC in aqueous solution becomes 20 mM which is well above their CMC values. Afterwards, different amounts of cholesterol were added into each glass bottle in order to vary the cholesterol content in terms of R values (R = cholesterol/[C_{16}mim]Cl molar ratio = (*Conc. of cholesterol*)/(*Conc.of* [C_{16}*mim*]*Cl*) from 0 to 1.5. Finally the resulting mixtures were sonicated using an ultrasonic probe sonicator (Oscar Ultrasonic) for 15 min at 298 K to obtain the vesicular solutions.

dx.doi.org/10.1021/jp501033n | J. Phys. Chem. B 2014, 118, 5913−5923

2.3. Turbidity Measurements. The turbidity of $[C_{16}mim]Cl$/cholesterol and BHDC/cholesterol solutions as a function of increasing cholesterol content (R) were measured using a Shimadzu (model no.UV-2450) absorption spectrophotometer. The wavelength for the measurement of optical density was selected to be 500 nm where there is no absorption of the individual components.

2.4. Dynamic Light Scattering (DLS) Measurements. Dynamic light scattering (DLS) measurements were performed using a Malvern Nano ZS instrument employing a 4 mW He−Ne laser (λ = 632.8 nm) and equipped with a thermostatic sample chamber. In the Malvern Zetasizer Nano ZS DLS instrument, the detector angle is fixed at 173° and we have used this instrument for DLS measurement. In DLS measurements the used water was first filtered through a syringe filter (0.2 μm) to make solutions dust-free. All measurements were performed at 298 K. (The experimental error in the DLS measurement of $[C_{16}mim]Cl$ and BHDC micelles is ±0.3 nm.)

2.5. Transmission Electron Microscopy Measurements. Transmission electron microscopy (TEM) analysis was carried out for the structural characterization of $[C_{16}mim]$-Cl/cholesterol and BHDC/cholesterol vesicles at different R values by using the JEOL model JEM 2010 transmission electron microscope at an operating voltage of 200 kV. TEM images of the vesicles were taken by using 0.5 wt % of uranyl acetate as the staining agent.

2.6. NMR Measurements. The ^1H NMR spectra of $[C_{16}mim]Cl$/cholesterol and BHDC/cholesterol solutions of varying cholesterol content (R = 0 to 1) were recorded using a Brüker 400 MHz NMR spectrometer. All NMR measurements were carried out in D_2O (Aldrich, 99.6 atom % D) solvent as the chemical shift reference for mode locking.

2.7. Steady-State Fluorescence Anisotropy Measurements. The steady-state fluorescence anisotropy values of a membrane bound probe DPH in the vesicular solutions with increasing cholesterol content were measured using a PerkinElmer LS-55 spectrofluorimeter. The steady-state anisotropy can be determined by using the following equation:

$$r = \frac{(I_{VV} - GI_{VH})}{(I_{VV} + 2GI_{VH})} \quad (1)$$

$$G = \frac{I_{HV}}{I_{HH}} \quad (2)$$

where I_{VV} and I_{VH} are the emission intensities of the sample when the excitation polarizer is oriented vertically and the emission polarizer is vertically and horizontally oriented, respectively. G is the correction factor for the sensitivity of the detector to the polarization direction of the emission.

2.8. Steady-State and Time-Resolved Fluorescence Studies. Shimadzu (model UV 2450) UV−vis spectrophotometer and Hitachi (Model No. F-7000) spectrofluorimeter were used to record steady-state UV−vis absorption and fluorescence emission spectra, respectively. A time correlated single photon counting (TCSPC) setup was used to collect time-resolved emission decays at the excitation wavelength of 408 nm. The detailed experimental setup of this instrument has been described in our previous publication.[52] The signal was detected in magic angle (54.7°) polarization using a Hamamatsu MCP PMT (3809U). The typical instrument response function that is the full width at half-maximum is ~90 ps in our system. The decays were analyzed using IBH DAS-6 decay analysis software.

For the anisotropy decays, we used a motorized polarizer in the emission side to collect the emission intensities at parallel ($I_{\parallel}$) and perpendicular ($I_{\perp}$) polarizations until a certain counts difference between parallel ($I_{\parallel}$) and perpendicular ($I_{\perp}$) decay was reached. The following equation is used to calculate the anisotropy value:

$$r(t) = \frac{I_{\parallel}(t) - GI_{\perp}(t)}{I_{\parallel}(t) + 2GI_{\perp}(t)} \quad (3)$$

where G is the correction factor for detector sensitivity to the polarization direction of the emission. For our experimental setup, the value of the G factor is 0.6 at the excitation wavelength of 408 nm.

3. RESULTS AND DISCUSSION

3.1. Characterization of $[C_{16}mim]Cl$/Cholesterol and BHDC/Cholesterol Vesicles. *3.1.1. Turbidity Measurements.* To understand the extent of turbidity, we measured the optical density of the solutions at a fixed wavelength of 500 nm where both of the components have no absorbance. The variation of optical density at 500 nm with increasing R of $[C_{16}mim]Cl$/cholesterol and BHDC/Cholesterol solutions are shown in Figure 1a and 1b. At R = 0 when there is no cholesterol, the optical density values of both $[C_{16}mim]Cl$ and BHDC micellar solutions are near 0. The optical density of the solution gradually increases as the R value gradually increases from 0 to 1. The gradual increase in the turbidity with an increase in the concentration of cholesterol can be better understood from the images of $[C_{16}mim]Cl$/cholesterol solutions given in Figure S1 (Supporting Information). This type of steep variation in the turbidity of solutions is quite expected for micelle−vesicle transitions. In each plot we observed a point of inflection which indicates the onset of vesicle formation from a micelle. Our

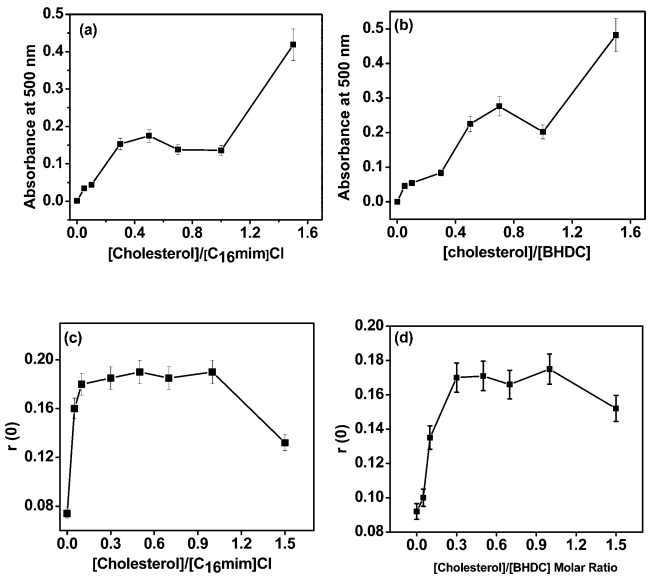

Figure 1. (a and b) Variation of absorbance at 500 nm of (a) $[C_{16}mim]Cl$/cholesterol and (b) BHDC/cholesterol self-assembled solutions with increasing R values. (c and d) Variation of steady-state anisotropy of DPH in the (c) $[C_{16}mim]Cl$/cholesterol and (d) BHDC/cholesterol self-assembled solutions with increasing R values.

dx.doi.org/10.1021/jp501033n | J. Phys. Chem. B 2014, 118, 5913−5923

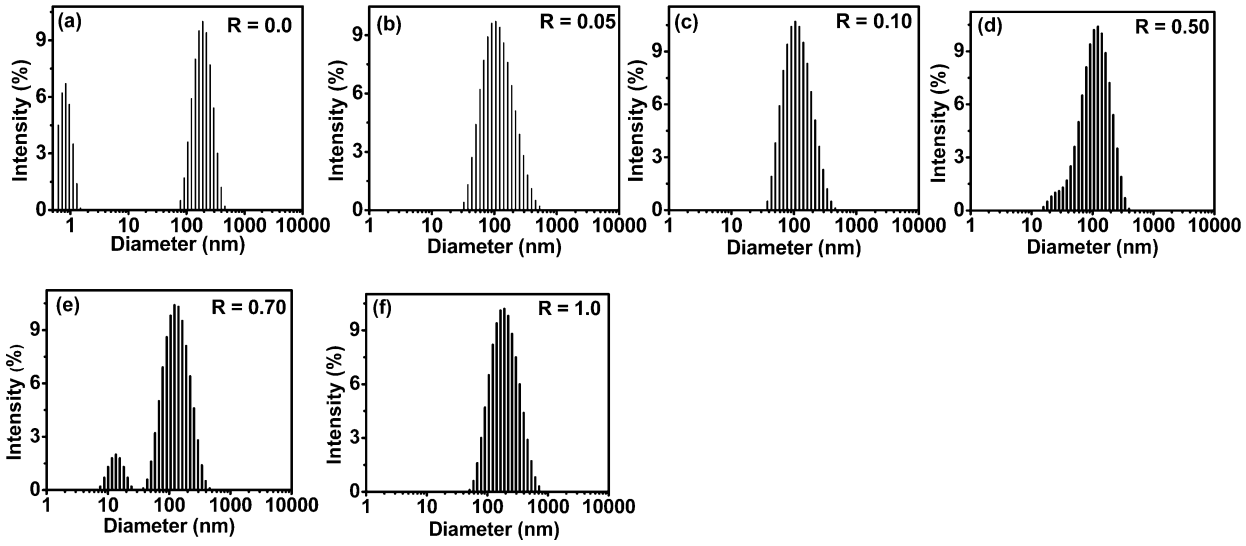

Figure 2. Size distributions of $[C_{16}mim]Cl$/cholesterol forming supramolecular assemblies at different cholesterol/$[C_{16}mim]Cl$ molar ratios (R): (a) 0.0, (b) 0.05, (c) 0.10, (d) 0.50, (e) 0.70, and (f) 1.0.

results indicate that the onset of vesicle formation appears at a lower R value in the $[C_{16}mim]Cl$/cholesterol system than in the BHDC/cholesterol system. This is due to the greater surface activity of imidazolium-based SAILs compared to conventional surfactants. Galgano et al.[26] have investigated the micellar properties of $[C_{16}mim]Cl$ and compared the results with those of structurally related conventional cationic surfactants. They have indicated that the basic difference between imidazolium-based SAILs with common surfactants is the nature of the headgroup. The headgroups of SAILs impart stronger hydrogen bonding ability to the counterions due to the presence of acidic protons of the imidazolium ring. Therefore, we can expect a higher extent of synergistic interaction of hydroxyl group of cholesterol with the headgroup of SAILs than with BHDC. This is further supported by the lower value of turbidity of $[C_{16}mim]Cl$/cholesterol vesicles than BHDC/cholesterol vesicles. The optical density is found to be abruptly increased at $R > 1$ in both systems due to the formation of larger aggregates. At very high R values, solid particles were found to be precipitated out from the dispersion.

3.1.2. Steady-State Anisotropy Studies. Micelle−vesicle transitions of the solutions were further indicated by the steady-state fluorescence anisotropy studies. The steady-state fluorescence anisotropy of both $[C_{16}mim]Cl$/cholesterol and BHDC/cholesterol solutions with increasing R value were measured using 1,6-diphenyl-1,3,5-hexatriene (DPH) as a fluorescent probe. DPH is particularly known as a membrane bound probe widely used to understand the rigidity of the membrane.[36] As micelles are gradually transformed into vesicles upon increasing concentration of cholesterol, the anisotropy values were found to be increased. This observation clearly indicates that the surrounding microenvironment of DPH in micelles is less rigid compared to that in vesicles. The higher the value of anisotropy, the higher the extent of incorporation of the probe into the rigid and confined microenvironments of vesicular bilayer. The dependence of the anisotropy value of DPH with R value in $[C_{16}mim]Cl$/cholesterol and BHDC/cholesterol solutions is shown in Figure 1c and 1d. In correlation with the results of turbidity measurement, here also we have observed that the sudden increase in the steady-state anisotropy value which roughly indicates the onset of micelle−vesicle transition appears at a lower R value in the $[C_{16}mim]Cl$/cholesterol system than in the BHDC/cholesterol system. Moreover, the steady state anisotropy values of $[C_{16}mim]Cl$/cholesterol vesicular solutions are found to be higher than that of BHDC/cholesterol vesicular solutions. This indicates that a higher level of interaction between cholesterol and $[C_{16}mim]Cl$ brings the higher extent of rigidity of the $[C_{16}mim]Cl$/Cholesterol bilayer than that of the BHDC/cholesterol bilayer. In both the systems the anisotropy value abruptly decreases at a very high value of R ($R = 1.5$) due to the formation of larger aggregates where the water accessibility to the bound probe increases.

The detailed mechanism of cholesterol induced micelle−vesicle transition in common cationic surfactant systems has already been reported in literature.[31,33] Ferrer-Tasies et al.[31] have indicated that the mechanism of cholesterol induced micelle−vesicle transition in a cationic surfactant system such as CTAB is quite different from that in the mixture of cationic and anionic surfactant systems. By MD simulation studies they have suggested that vesicles are formed by the synergistic interaction between cholesterol and cationic surfactants and thereby produce a bimolecular synthon which at a certain molar ratio behaves as a single component for the formation of vesicles. In the case of cholesterol-based vesicles cholesterol remains in the interior of the bilayer and enhances the hydrophobicity.[31−34] Initially, at very low cholesterol content ($R < 0.1$) mixed micelles are preferentially formed through the encapsulation of cholesterol molecules into the $[C_{16}mim]Cl$ micelle or BHDC micelles. With further increases in the cholesterol concentration, mixed micelles are converted into vesicles. The formation of a vesicle is confirmed by the sudden increase in the value of optical density of the solution as well as the steady-state anisotropy of DPH as a result of binding with the bilayer membrane of vesicles (Figure 1). However, at very high cholesterol content (when $R > 1.0$), there are very few surface active components compared to cholesterol molecules, and thereby at this state excess cholesterol molecules start to be precipitated out.

3.1.3. Dynamic Light Scattering Studies. Dynamic light scattering measurements were carried out to measure the change in the size of the aggregates for micelle−vesicle

dx.doi.org/10.1021/jp501033n | J. Phys. Chem. B 2014, 118, 5913−5923

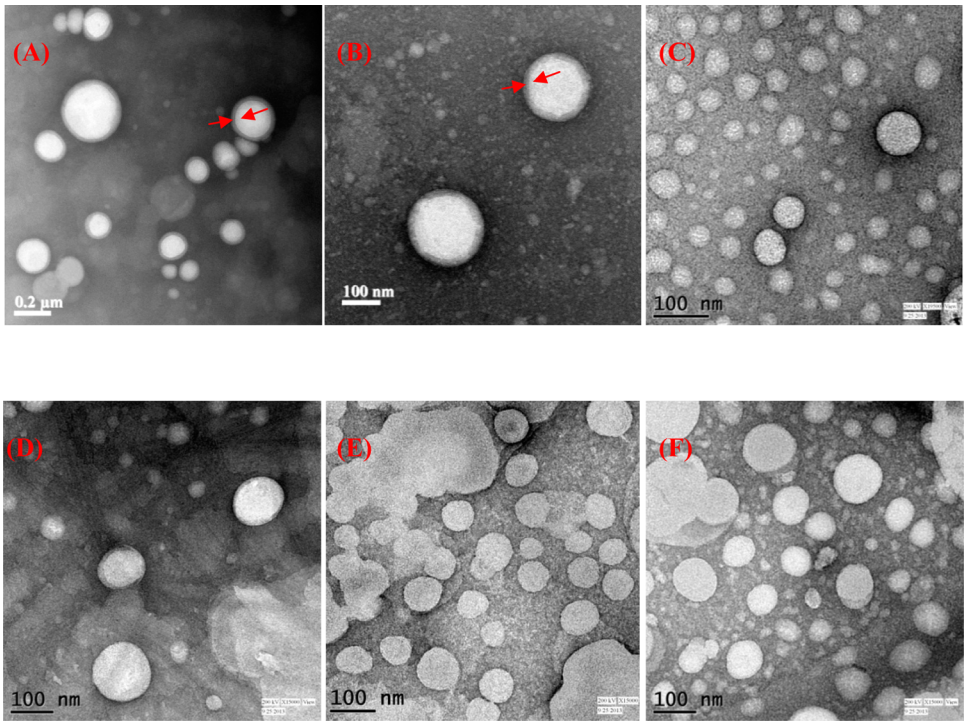

Figure 3. (A–C) TEM images of $[C_{16}mim]Cl$/cholesterol vesicles at different R values of (A) 0.1, (B) 0.5, and (C) 1.0. (Red arrows indicate the presence of bilayer region.) (D–F) TEM images of BHDC/cholesterol vesicles at different R values (D) 0.1, (E) 0.5, and (F) 1.0.

transitions into the aqueous solutions of $[C_{16}mim]Cl$ and BHDC solutions upon increasing concentration of cholesterol. The size distributions of $[C_{16}mim]Cl$/cholesterol aggregates at different R values are shown in Figure 2, while that of BHDC/cholesterol aggregates are shown in Figure S2 (Supporting Information). At R = 0, the hydrodynamic diameter of $[C_{16}mim]Cl$ micelles as obtained from DLS measurement is ∼1 nm. Another peak of minor populations at 150 nm is also observed which is probably due to the formation of larger $[C_{16}mim]Cl$ aggregates. Similar results are also observed for the DLS measurement of the aqueous common cationic surfactant CTAB as reported by Ferrer-Tasies et al.[31] The size of the aggregates increases with increasing cholesterol content due to structural transitions of micelles to mixed micelles, elongated micelles, and vesicles. At lower R values we observed the presence of both micelles and vesicles together in the solutions. Since the light scattering intensity is proportional to the sixth power of the diameter of the particles, at very low cholesterol content the populations of the smaller micelles are not detected. At R = 0.05 and 0.1 the size distribution profiles are found to be monomodal with a low polydispersity index suggesting the presence of spherical aggregates. The diameters of the aggregates are found to be ∼100 nm in this range of R values. At R = 0.5 and 0.7 values the size distribution profiles are found to be slightly distorted due to the formation of large aggregates. However, as the R value is further increased to 1.0, only a single distribution of the hydrodynamic diameter of ∼150 nm is observed. The variation in the size distribution of BHDC/cholesterol assemblies with increasing R value also follows a similar kind of trend as it follows in the $[C_{16}mim]Cl$/cholesterol system. The average hydrodynamic diameter of BHDC/cholesterol vesicles remains in the range of 100–150 nm. The present results are consistent with the earlier observations of micelle–vesicle transitions in the mixture of cholesterol and common surfactants. Using molecular dynamics simulations studies, Ferrer-Tasies et al.[31] indicated that at the equimolar mixture of CTAB and cholesterol the system contains a pure phase of spherical and unilamellar vesicles. Therefore, we can infer that in a certain range of R values from R = 0 to 1.0, with the increase in the concentration of cholesterol a higher number of micelles are transformed into vesicles and finally at R = 1.0 a uniform distribution of spherical unilamerllar vesicles are obtained. Therefore, DLS results along with the turbidity and anisotropy studies have indicated the formation of spherical vesicles from $[C_{16}mim]Cl$ ionic liquid and BHDC surfactant at different concentrations of cholesterol. It is noteworthy to mention that both $[C_{16}mim]Cl$/cholesterol and BHDC/cholesterol vesicles at R = 1.0 were found to be stable for almost one year without any significant change in the DLS size distribution profiles when stored at 298 K.

3.1.4. Transmission Electron Microscopy (TEM) Measurements. The microstructure of the aggregates at varying cholesterol content can be better understood from the TEM analysis. Figure 3 represents the TEM images of the $[C_{16}mim]Cl$/cholesterol and BHDC/cholesterol vesicles at three different R values (0.1, 0.5, and 1.0). From the TEM images of both systems, we can see the existence of spherical vesicles at each and every different R value ranging from 0.1 to 1.0. Moreover, the sizes of the vesicles are consistent with the sizes obtained from DLS measurements. The presence of a distinct bilayer region is clearly observed from the TEM images of $[C_{16}mim]Cl$/cholesterol vesicles as indicated by red arrows in Figure 2 A and 2B. As we said earlier, at lower values of R, micellar aggregates coexist along with the comparatively larger aggregates of unilamellar vesicles. This was confirmed by the TEM images of $[C_{16}mim]Cl$/cholesterol and BHDC/cholesterol solutions at R = 0.1 and 0.5, where we can see the existence of spherical small sized particles for micelles along with the comparatively larger unilamellar vesicles. However, the

dx.doi.org/10.1021/jp501033n | J. Phys. Chem. B 2014, 118, 5913–5923

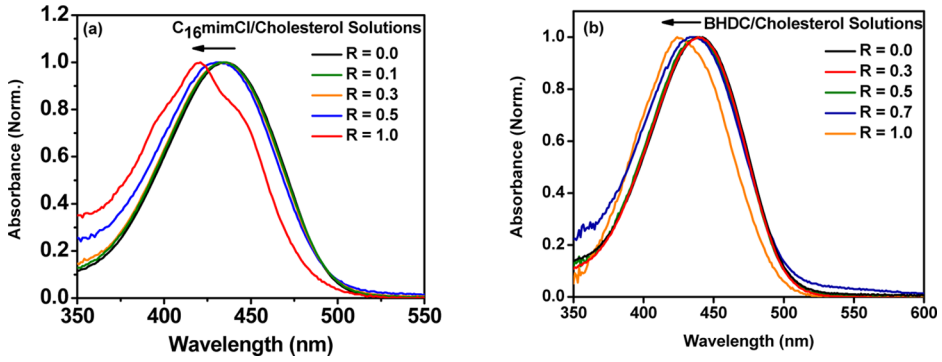

Figure 4. UV−vis absorption spectra of C153 in (a) [C_{16}mim]Cl/cholesterol and (b) BHDC/cholesterol solutions of varying cholesterol content in terms of *R* values.

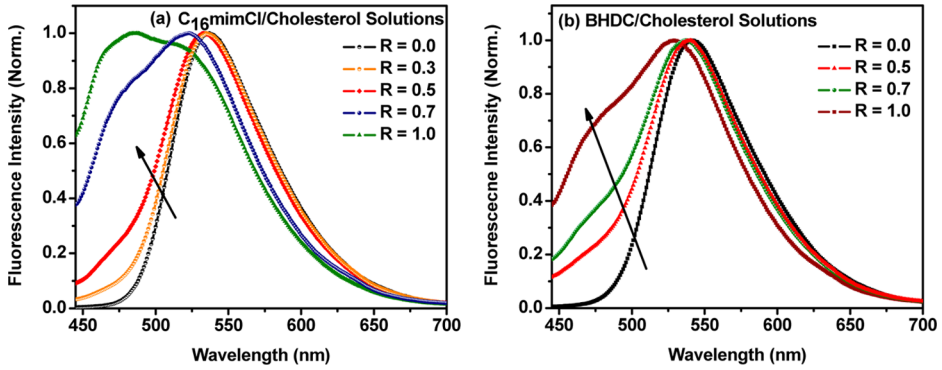

Figure 5. Steady-state fluorescence emission spectra of C153 in (a) [C_{16}mim]Cl/cholesterol and (b) BHDC/cholesterol solutions with increasing *R* values.

distribution of the vesicles becomes more uniform as the cholesterol content gradually increases up to $R = 1.0$.

3.1.5. NMR Studies. We have further applied ^{1}H NMR techniques to understand the structural transitions from micelles to vesicles upon interaction of cholesterol with [C_{16}mim]Cl and BHDC in deuterium oxide solutions of different *R* values. ^{1}H NMR measurement helps us to understand the synergistic interaction between the surface active material and cholesterol resulting in the formation of vesicles. Figure S3 (Supporting Information) shows the changes in the NMR spectra of [C_{16}mim]Cl/cholesterol solutions as a function of increasing cholesterol content. From this figure we can see that the NMR peaks responsible for the protons in the alkyl chain of [C_{16}mim]Cl are significantly broadened as micelles are transformed in vesicles upon gradual addition of cholesterol. We have also observed that the doublet NMR peak for the aromatic protons of [C_{16}mim]Cl at C-4 and C-5 positions gradually merged into a single broad peak in the vesicular solutions. Similar types of changes are also observed in BHDC/cholesterol system. The formation of compact self-assembled structures, such as vesicles, often leads to peak broadening due to the restricted movement and shorter relaxation times of nuclei.[30] The broadening of the aromatic as well as alkyl proton of [C_{16}mim]Cl indicates the involvement of a cationic part of [C_{16}mim]Cl with a cholesterol in the self-assembly. Basically, a balanced interaction between headgroups, alkyl chains of both cholesterol and [C_{16}mim]Cl are responsible for the vesicle formation. Villeneuve et al.[58] reported on the vesicle−micelle transition in the aqueous mixture of common cationic and anionic surfactants by ^{1}H NMR relaxation measurement. They have indicated that the broadening of the peaks in vesicular solutions generally arises from various curvatures of the multiply bilayered vesicles, the liquid-crystal-like nature in the vesicle interior, and polydisperse distribution of the vesicular size.

3.2. Solvation and Rotational Dynamics Studies.

3.2.1. Steady-State Studies. Figure 4 shows the absorption spectra of C153 in [C_{16}mim]Cl/cholesterol and BHDC/cholesterol solutions at different *R* values. In the aqueous [C_{16}mim]Cl and BHDC micellar solutions, the emission maxima of C153 appear at 437 and 442 nm, respectively. As the concentration of cholesterol increases the absorption maxima gradually blue-shifted indicating the gradual incorporation of the probe molecules into the hydrophobic bilayer region of vesicles. This is obviously the consequence of cholesterol induced micelles to vesicles transition in the aqueous solutions of both [C_{16}mim]Cl and BHDC. The absorption maxima of C153 show only a little shift up to $R = 0.5$. However, at a higher concentration of cholesterol ($R = 1.0$) the absorption maxima shift dramatically by 15−18 nm in the blue region. It has been proposed that, at $R = 1.0$, the system contains only vesicles, and therefore, at this composition we may expect a more rigid and hydrophobic microenvironment surrounding the probe molecules, thereby resulting in more significant spectral changes. It is noteworthy to mention that we observed a more prominent change (blue shift) in the spectral feature of the absorption spectra of C153 in [C_{16}mim]Cl/cholesterol solution than in BHDC/cholesterol solution at the $R = 1.0$ value. The observation of vibronic structure in the absorption spectra as well as the higher extent of blue shift in the absorption maxima of C153 in the [C_{16}mim]Cl/cholesterol system at $R = 1.0$ clearly indicate that the bilayer of the

dx.doi.org/10.1021/jp501033n | J. Phys. Chem. B 2014, 118, 5913−5923

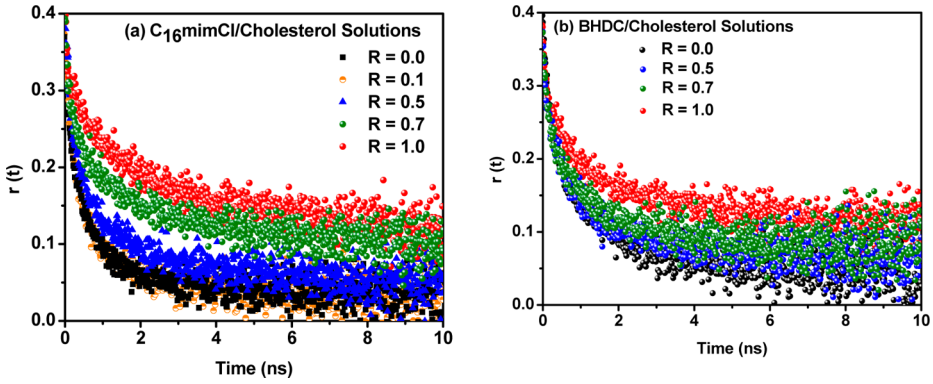

Figure 6. Time-resolved fluorescence anisotropy decays of C153 in (a) [C_{16}mim]Cl/cholesterol and (b) BHDC/cholesterol solutions with increasing *R* value.

[C_{16}mim]Cl/cholesterol vesicle provides comparatively a more hydrophobic microenvironment than that provided by the bilayer of BHDC/cholesterol vesicles.

Understanding the differences between [C_{16}mim]Cl/cholesterol and BHDC/cholesterol vesicular assemblies appears to be very crucial if we compare their extent of rigidity and hydration behavior from the fluorescence spectroscopy studies. The steady-state fluorescence spectra of C153 in [C_{16}mim]Cl/cholesterol and BHDC/cholesterol solutions of varying cholesterol content are shown in Figure 5. In [C_{16}mim]Cl and BHDC micellar solutions the emission maxima of C153 appear at 537 and 542 nm, respectively. With increasing cholesterol content of the solutions the emission spectra are blue-shifted suggesting an increase in the hydrophobicity of the surrounding microenvironment. However, the extent of blue shift in the emission maxima is found to be higher in the case of [C_{16}mim]Cl/cholesterol vesicular solutions than in BHDC/cholesterol vesicular solutions. At $R = 0.7$, the emission maxima of C153 in [C_{16}mim]Cl/cholesterol appear at 523 nm while in BHDC/cholesterol solution it appears at 530 nm. This observation is in correlation with the observation of UV−vis absorption studies.

Apart from the blue shift in the emission maxima, we also observed the existence of a shoulder band at ∼478 nm at higher *R* values. The intensity of this shoulder band gradually increases as the cholesterol content increases beyond $R = 0.5$ for the [C_{16}mim]Cl/cholesterol system and $R = 0.7$ for the BHDC/cholesterol system. It has been earlier shown that the presence of cholesterol increases the hydrophobicity and rigidity of the bilayer region of vesicles. At the equimolar mixture of [C_{16}mim]Cl and cholesterol, i.e. at $R = 1.0$, the distribution of the vesicles become uniform and in this situation the highest extent of confinement of C153 in the hydrophobic bilayer regions is most likely to occur. Interestingly, at $R = 1.0$, the emission spectra of C153 in both systems are found to be broadened with a huge blue shift of the emission maxima. The broadness of the emission spectra probably arises from the multiple locations of C153 in the vesicular assemblies. This unique spectral feature can also be attributed to the presence of C153 aggregates in the vesicular bilayer because similar types of emission spectra were earlier reported by Bhattacharyya et al.[59] for the aggregation of C153 in 105 mM of bile salt aggregates. Therefore, the present observation is not surprising as both bile salt and cholesterol contain almost similar steroidal skeletons with the difference being only in the headgroup region.

The most interesting observation is that, at $R = 1.0$, the emission spectral feature of C153 in [C_{16}mim]Cl/cholesterol vesicles is significantly different from that in BHDC/cholesterol vesicles. This is obviously due to the difference in the hydration behavior and rigidity between [C_{16}mim]Cl/cholesterol and BHDC/cholesterol self-assemblies. We can see that, at $R = 1.0$, while the intensity of the emission band at 478 nm which is responsible for the strong confinement of the probe molecule in the hydrophobic bilayer region becomes a maximum in [C_{16}mim]Cl/cholesterol system, this band remains as a shoulder band of lesser intensity in the BHDC/cholesterol system. This observation further supports that the bilayer of [C_{16}mim]Cl/cholesterol vesicles is comparatively less hydrated and more rigid than that of BHDC/cholesterol vesicles.

3.2.2. Time-Resolved Anisotropy Studies. To further understand the increased rigidity and hydrophobicity of the surrounding microenvironment of the probe in the course of micelle−vesicle transitions, we performed time-resolved fluorescence anisotropy studies. Figure 6 shows the changes in the anisotropy decay of C153 during the microstructural transition of micelles to vesicles in [C_{16}mim]Cl/cholesterol and BHDC/cholesterol solutions. In all solutions, the anisotropy decays of C153 fit well to a biexponential function and the corresponding fitted decay parameters are given in Table 1. In aqueous solutions the anisotropy decay of C153 is single exponential with a time constant of ∼100 ps.[50] However, in micellar solutions the decays become bimodal in nature with longer rotational relaxation time constants due to the confinement of the probe molecules in micelles. The anisotropy decay of C153 becomes gradually slower with increasing concentration of cholesterol in the aqueous solution of both [C_{16}mim]Cl and BHDC. This observation confirms that as micelles are transformed into vesicles upon addition of cholesterol, the probe molecules are incorporated into the rigid and confined microenvironments of the vesicles. Due to the strong hydrophobicity and poor aqueous solubility of C153, the probe molecules preferentially reside in the hydrophobic bilayer region of the vesicles. As the bilayer of the [C_{16}mim]Cl/cholesterol vesicle are more rigid than the bilayer of BHDC/cholesterol vesicles, we observed a comparatively higher extent of increase in the rotational relaxation upon micelle−vesicle transition in [C_{16}mim]Cl/cholesterol than in the BHDC/cholesterol system.

Note that the anisotropy of C153 in both [C_{16}mim]Cl/cholesterol and BHDC/cholesterol solutions of high cholesterol content ($R = 0.7$ and 1.0) does not decay to zero over 10 ns

dx.doi.org/10.1021/jp501033n | J. Phys. Chem. B 2014, 118, 5913−5923

Table 1. Time-Resolved Anisotropy Decay Parameters of C153 in [C_{16}mim]Cl/Cholesterol and BHDC/Cholesterol Solutions at Different *R* Values

systems	a_{1r}	τ_{1r} (ns)	a_{2r}	τ_{2r} (ns)	$\langle\tau_r\rangle^a$ (ns)
C153 in [C_{16}mim]Cl micelles (R = 0)	0.58	0.29	0.42	1.26	0.70
C153 in [C_{16}mim]Cl/cholesterol solution R = 0.1	0.56	0.27	0.44	1.36	0.75
C153 in [C_{16}mim]Cl/cholesterol solution R = 0.5	0.56	0.29	0.44	1.86	0.98
C153 in [C_{16}mim]Cl/cholesterol solution R = 0.7	0.50	0.17	0.50	1.96	1.07
C153 in [C_{16}mim]Cl/cholesterol solution R = 1.0	0.43	0.10	0.57	2.29	1.35
C153 in BHDC micelles	0.48	0.22	0.52	1.51	0.89
C153 in BHDC/cholesterol solution R = 0.5	0.49	0.33	0.51	1.66	1.00
C153 in BHDC/cholesterol solution R = 0.7	0.48	0.32	0.52	1.81	1.10
C153 in BHDC/cholesterol solution R = 1.0	0.44	0.40	0.56	2.27	1.45

$^a\langle\tau_r\rangle = a_1\tau_1 + a_2\tau_2$ for biexponential fluorescence anisotropy decays where, τ_1 and τ_2 are the rotational time constants with their corresponding relative amplitude a_1 and a_2. Experimental error ±5%.

(see Figure 6). This indicates that in these vesicular solutions the rotational motions of the confined probe molecules are strongly hindered. This residual anisotropy may also arise from the aggregation of the probe molecules in the bilayer region of the vesicles. A similar kind of anisotropy decay with residual anisotropy over 20 ns is also reported to be observed for C153 in 40 mM of γ-cyclodextrin solution due to the formation of linear aggregates of the probe molecules upon complexation with cyclodextrins.[60]

3.2.3. Solvation Dynamics Study. Solvation dynamics has been extensively studied over the past few decades as a sensitive method for better understanding the hydration behavior of various biological assemblies. Here, we have shown the changes in the hydration behavior of the biologically relevant self-assemblies upon micelle−vesicle transitions by monitoring the dynamical behavior of C153.[61] For this purpose we have collected the emission decays of C153 in [C_{16}mim]Cl/cholesterol and BHDC/cholesterol solutions of varying cholesterol content (R value vary from 0 to 1) at several emission wavelengths. Then from the parameters of best fit to the fluorescence decays, the time-resolved emission spectra (TRES) were constructed following the procedure of Fleming and Maroncelli.[57] The TRES at a given time t, $S(\lambda;t)$, is obtained by the fitted decays, $D(t;\lambda)$, by relative normalization to the steady-state spectrum $S_0(\lambda)$, as follows

$$S(\lambda;\, t) = D(\lambda;\, t)\frac{S_0(\lambda)}{\int_0^\infty D(\lambda;\, t)\, dt} \tag{4}$$

Each (TRES) was fitted by "log-normal line shape function", which is defined as

$$g(\nu) = g_0 \exp\left[- \ln 2\left(\frac{\ln[1 + 2b(\nu - \nu_p)]/\Delta}{b}\right)^2\right] \tag{5}$$

where g_0, b, ν_p, and Δ are the peak height, asymmetric parameter, peak frequency, and width parameter, respectively. The TRES plot of C153 in the [C_{16}mim]Cl/cholesterol system at R = 0.5 is shown in Figure S4 of the Supporting Information as a representative example. We have calculated the peak frequency from the log-normal fitting of TRES. This peak frequency is used to construct the decay of the solvent correlation function $C(t)$, which is defined as

$$C(t) = \frac{\upsilon(t) - \upsilon(\infty)}{\upsilon(0) - \upsilon(\infty)} \tag{6}$$

where $\upsilon(0)$, $\upsilon(t)$, and $\upsilon(\infty)$ are the peak frequency at time zero, t, and infinity. The decays of $C(t)$ are fitted by a biexponential function:

$$C(t) = a_1 \exp^{-t/\tau_1} + a_2 \exp^{-t/\tau_2} \tag{7}$$

where τ_1 and τ_2 are the solvation times with amplitudes of a_1 and a_2, respectively.

The decays of $C(t)$ for C153 in [C_{16}mim]Cl/cholesterol and BHDC/cholesterol solutions with increasing R are shown in Figure 7, and the fitted decay parameters are given in Table 2. It can be seen that as the R value increases from 0 to 1 the decay of $C(t)$ becomes gradually slower. In [C_{16}mim]Cl micelles the decay of $C(t)$ consists of two components of 170 and 290 ps with an average solvation time of 240 ps. In contrast, in BHDC micelles we observed an average solvation time of 380 ps consisting of a fast component of 190 ps and a slow component of 500 ps. Therefore, it is important to note that the solvation dynamics in ionic liquid micelles is faster than that in common surfactant forming micelles having the difference only in the headgroup region. This observation is in complete agreement with the earlier literature reports.[51,52] Seth et al.[52] reported earlier that the solvation dynamics of C153 in [C_4mim]-

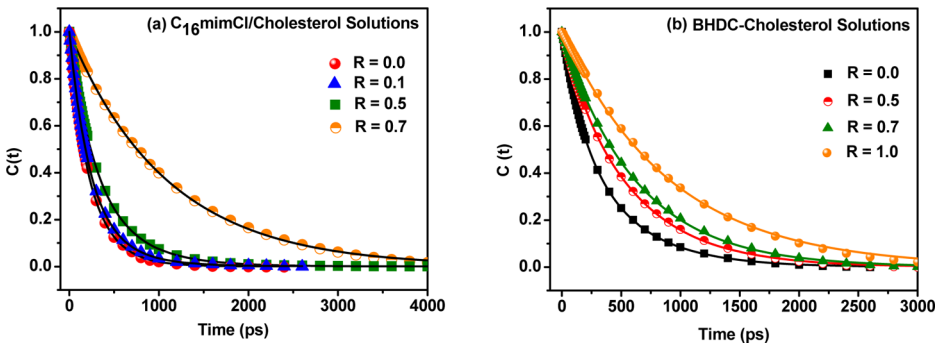

Figure 7. Decay plots of solvent correlation function ($C(t)$) of C153 in (a) [C_{16}mim]Cl/cholesterol and (b) BHDC/cholesterol solutions at different R values ranging from 0 to 1.

dx.doi.org/10.1021/jp501033n | J. Phys. Chem. B 2014, 118, 5913−5923

Table 2. Decay Parameters of $C(t)$ of C153 in $[C_{16}mim]Cl$/Cholesterol and BHDC/Cholesterol Solutions at Different R Values

systems	a_1	τ_1 (ns)	a_2	τ_2 (ns)	$\langle\tau_s\rangle^a$ (ns)
C153 in $[C_{16}mim]Cl$ micelles	0.43	0.17	0.57	0.29	0.24
C153 in $[C_{16}mim]Cl$/cholesterol solution R = 0.1	0.77	0.22	0.23	0.46	0.28
C153 in $[C_{16}mim]Cl$/cholesterol solution R = 0.5	0.61	0.27	0.39	0.54	0.38
C153 in $[C_{16}mim]Cl$/cholesterol solution R = 0.7	0.04	0.18	0.96	1.13	1.09
C153 in BHDC micelles R = 0	0.39	0.19	0.61	0.50	0.38
C153 in BHDC/cholesterol solution R = 0.5	0.28	0.32	0.72	0.63	0.54
C153 in BHDC/cholesterol solution R = 0.7	0.35	0.52	0.65	0.70	0.64
C153 in BHDC/cholesterol solution R = 1.0	–	–	1.00	0.90	0.90

$^a\langle\tau_s\rangle = a_1\tau_1 + a_2\tau_2$ for biexponential decays of $C(t)$, where τ_1 and τ_2 are the solvent relaxation time constants with their corresponding relative amplitude a_1 and a_2. Experimental error ±5%.

$[C_8SO_4]$ micelles is faster than the solvation dynamics in $C_8H_{17}SO_4Na$ micelles although both micelle forming components have the same alkyl chain length. Now, with an increase in concentration of cholesterol, the average solvation time gradually increases due to the decrease in the hydration behavior surrounding the probe molecule as micelles are transformed into vesicles. In the vesicular solutions (R = 0.7–1.0), the solvation time is found to be 3–5 times higher than that in micelles (R = 0). For the two different types of vesicular solutions, we have observed that the extent of increase in solvation time upon vesicle transition (R = 0.0–1.0) is significantly higher in the $[C_{16}mim]Cl$/cholesterol system than in the BHDC/cholesterol system (Table 2). This indicates that the hydration behavior of $[C_{16}mim]Cl$/cholesterol vesicles is comparatively less than that of BHDC/cholesterol vesicles. The bimodal decay kinetics of $C(t)$ of C153 in micelles and vesicles can be better understood from the dynamic exchanges model proposed by Nandi and Bagchi.[44] According to this model the dynamic between free and bound water molecules in the confined system is responsible for two types of decay components, namely fast and slow components.

4. CONCLUSION

This work demonstrates the formation of cholesterol-based supramolecular vesicles from an imidazolium surface active ionic liquid, $[C_{16}mim]Cl$. We have shown that addition of cholesterol at different R values in the aqueous micellar solution of $[C_{16}mim]Cl$ results in the transformation of micelles to unilamellar vesicles. In order to generalize and compare, we have also shown that cholesterol induced such micelle–vesicle transitions in the micellar solution of a common cationic surfactant, with BHDC having a similar alkyl chain length but different headgroup region compared to those of $[C_{16}mim]Cl$. The formation of vesicles with a distinct bilayer region has been confirmed with the help of DLS, TEM, UV–vis absorption spectroscopy and steady-state fluorescence anisotropy methods. These unilamellar vesicles are found to be stable for more than a year and therefore can be stored for a long period. From the solvation dynamics study it has been revealed that as micelles are transformed into vesicles a 3–5-fold increase occurs in the solvation time due to the decrease in the hydration behavior. Overall results also suggest that $[C_{16}mim]Cl$/cholesterol vesicles are comparatively more rigid and hydrophobic than BHDC/cholesterol vesicles. Finally, we can say that these newly developed stable supramolecular $[C_{16}mim]Cl$/cholesterol and BHDC/Cholesterol vesicles are expected to have great potential in the applications of controlled release and drug delivery.

■ ASSOCIATED CONTENT

Supporting Information

Information on the time-resolved emissions spectra (TRES) of C153 in $[C_{16}mim]Cl$/cholesterol vesicular solution at R = 0.5. This material is available free of charge via the Internet at http://pubs.acs.org.

■ AUTHOR INFORMATION

Corresponding Author

*E-mail: nilmoni@chem.iitkgp.ernet.in. Fax: 91-3222-255303.

Notes

The authors declare no competing financial interest.

■ ACKNOWLEDGMENTS

N.S. is thankful to the Council of Scientific and Industrial Research (CSIR), Government of India, for generous research grants. S.M. and S.G. are thankful to the CSIR for research fellowships. C.B. and J.K. are thankful to UGC for research fellowships.

■ REFERENCES

(1) Lian, T.; Ho, R. J. Trends and Developments in Liposome Drug Delivery Systems. *J. Pharm. Sci.* **2001**, *90*, 667–680.

(2) Medinai, O. P.; Zhu, Y.; Kairemo, K. Targeted Liposomal Drug Delivery in Cancer. *Curr. Pharm. Des.* **2004**, *10*, 2981–2989.

(3) Nabel, G. L.; Nabel, E. G.; Yang, Z.; Fox, B. A.; Plautz, G. E.; Gao, X.; Huang, L.; Shu, S.; Gordon, D.; Chang, A. E. Direct Gene Transfer with DNA Liposome Complexes in Melanoma: Expression, Biological Activity, Lack of Toxicity in Humans. *Proc. Natl. Acad. Sci. U.S.A.* **1993**, *90*, 11307–11311.

(4) Onyesom, I.; Lamprou, D. A.; Sygellou, L.; Owusu-Ware, S. K.; Antonijevic, M.; Chowdhry, B. Z.; Douroumis, D. Sirolimus Encapsulated Liposomes for Cancer Therapy: Physicochemical and Mechanical Characterization of Sirolimus Distribution within Liposome Bilayers. *Mol. Pharmaceutics* **2013**, ASAP (DOI: 10.1021/mp400362v).

(5) Dubois, M.; Zemb, T. Phase-Behavior and Scattering of Doublechain Surfactants in Diluted Aqueous-Solutions. *Langmuir* **1991**, *7*, 1352–1360.

(6) Kaler, E. W.; Murthy, A. K.; Rodriguez, B. E.; Zasadzinski, J. A. Spontaneous Vesicle Formation in Aqueous Mixtures of Single-Tailed Surfactants. *Science* **1989**, *245*, 1371–1374.

(7) Chandrawati, R.; Caruso, F. Biomimetic Liposome- and Polymersome-Based Multicompartmentalized Assemblies. *Langmuir* **2012**, *28*, 13798–13807.

(8) Tanner, P.; Baumann, P.; Enea, R.; Onaca, O.; Palivan, C.; Meier, W. Polymeric Vesicles: From Drug Carriers to Nanoreactors and Artificial Organelles. *Acc. Chem. Res.* **2011**, *44*, 1039–1049.

(9) Rhodes, D. G.; Blazek-Welsh, A.. *Proniosome-Derived Niosomes for the Delivery of Poorly Soluble Drugs*; ACS Symposium Series 879;. American Chemical Society: Washington, DC, 2004; pp 40–49.

(10) Tavano, L.; Muzzalupo, R.; Mauro, L.; Pellegrino, M.; Andó, S.; Picci, N. Transferrin-Conjugated Pluronic Niosomes as a New Drug Delivery System for Anticancer Therapy. *Langmuir* **2013**, *29*, 12638–12646.

(11) Liu, T.; Guo, R. Preparation of a Highly Stable Niosome and Its Hydrotrope-Solubilization Action to Drugs. *Langmuir* **2005**, *21*, 11034−11039.
(12) Schreier, H.; Bouwstra, J. Liposomes and Niosomes as Topical Drug Carriers: Dermal and Transdermal Drug Delivery. *J. Controlled Release* **1994**, *30*, 1−15.
(13) Mandal, S.; Banerjee, C.; Ghosh, S.; Kuchlyan, J.; Sarkar, N. Modulation of the Photophysical Properties of Curcumin in Nonionic Surfactant (Tween-20) Forming Micelles and Niosomes: A Comparative Study of Different Microenvironments. *J. Phys. Chem. B* **2013**, *117*, 6957−6968.
(14) Wang, H.; Wang, J.; Zhang, S. B.; Xuan, X. P. Structural Effects of Anions and Cations on the Aggregation Behavior of Ionic Liquids in Aqueous Solutions. *J. Phys. Chem. B* **2008**, *112*, 16682−16689.
(15) Zhao, Y.; Gao, S.; Wang, J.; Tang, J. Aggregation of Ionic Liquids [$C_n$mim]Br (n = 4, 6, 8, 10, 12) in D_2O: A NMR Study. *J. Phys. Chem. B* **2008**, *112*, 2031−2039.
(16) Shi, L.; Li, N.; Yan, H.; Gao, Y.; Zheng, L. Aggregation Behavior of Long-Chain N-Aryl Imidazolium Bromide in Aqueous Solution. *Langmuir* **2011**, *27*, 1618−1625.
(17) Shi, L.; Zheng, L. Aggregation Behavior of Surface Active Imidazolium Ionic Liquids in Ethylammonium Nitrate: Effect of Alkyl Chain Length, Cations, and Counterions. *J. Phys. Chem. B* **2012**, *116*, 2162−2172.
(18) Blesic, M.; Lopes, A.; Melo, E.; Petrovski, Z.; Plechkova, N. V.; Canongia Lopes, J. N.; Seddon, K. R.; Rebelo, L. P. N. On the Self-Aggregation and Fluorescence Quenching Aptitude of Surfactant Ionic Liquids. *J. Phys. Chem. B* **2008**, *112*, 8645−8650.
(19) Wang, X.; Wang, R.; Zheng, Y.; Sun, L.; Yu, L.; Jiao, J.; Wang, R. Interaction between Zwitterionic Surface Activity Ionic Liquid and Anionic Surfactant: Na^+-Driven Wormlike Micelles. *J. Phys. Chem. B* **2013**, *117*, 1886−1895.
(20) Ao, M.; Kim, D. Aggregation Behavior of Aqueous Solutions of 1-Dodecyl-3-methylimidazolium Salts with Different Halide Anions. *J. Chem. Eng. Data* **2013**, *58*, 1529−1534.
(21) Brown, P.; Butts, C. P.; Dyer, R.; Eastoe, J.; Grillo, I.; Guittard, F. d. r.; Rogers, S.; Heenan, R. Anionic Surfactants and Surfactant Ionic Liquids with Quaternary Ammonium Counterions. *Langmuir* **2011**, *27*, 4563−4571.
(22) Brown, P.; Butts, C. P.; Eastoe, J.; Fermin, D.; Grillo, I.; Lee, H.; Parker, D.; Plana, D.; Richardson, R. M. Anionic Surfactant Ionic Liquids with 1-Butyl-3-methyl-imidazolium Cations: Characterization and Application. *Langmuir* **2012**, *28*, 2502−2509.
(23) Rao, V. G.; Ghosh, S.; Ghatak, C.; Mandal, S.; Brahmachari, U.; Sarkar, N. Designing a New Strategy for the Formation of IL-in-Oil Microemulsions. *J. Phys. Chem. B* **2012**, *116*, 2850−2855.
(24) Mahajan, S.; Sharma, R.; Mahajan, R. K. An Investigation of Drug Binding Ability of a Surface Active Ionic Liquid: Micellization, Electrochemical, and Spectroscopic Studies. *Langmuir* **2012**, *28*, 17238−17246.
(25) Dong, B.; Zhang, J.; Zheng, L.; Wang, S.; Li, X.; Inoue, T. Salt-Induced Viscoelastic Wormlike Micelles Formed in Surface Active Ionic Liquid Aqueous Solution. *J. Colloids Interface Sci.* **2008**, *319*, 338−343.
(26) Galgano, P. D.; El Seoud, O. A. Micellar Properties of Surface Active Ionic Liquids: A Comparison of 1-Hexadecyl-3-methylimidazolium Chloride with Structurally Related Cationic Surfactants. *J. Colloid Interface Sci.* **2010**, *345*, 1−11.
(27) Wang, H.; Zhang, L.; Wang, J.; Lia, Z.; Zhang, S. The First Evidence for Unilamellar Vesicle Formation of Ionic Liquids in Aqueous Solutions. *Chem. Commun.* **2013**, *49*, 5222−5224.
(28) Gu, Y.; Shi, L.; Cheng, X.; Lu, F.; Zheng, L. Aggregation Behavior of 1-Dodecyl-3-methylimidazolium Bromide in Aqueous Solution: Effect of Ionic Liquids with Aromatic Anions. *Langmuir* **2013**, *29*, 6213−6220.
(29) Yua, J.; Bai, X.; Zhao, M.; Zheng, L. C_{12}mimBr Ionic Liquid/SDS Vesicle Formation and Use as Template for the Synthesis of Hollow Silica Spheres. *Langmuir* **2010**, *26*, 11726−11731.
(30) Rao, K. S.; Singh, T.; Kumar, A. Aqueous-Mixed Ionic Liquid System: Phase Transitions and Synthesis of Gold Nanocrystals. *Langmuir* **2011**, *27*, 9261−9269.
(31) Ferrer-Tasies, L.; Moreno-Calvo, E.; Cano-Sarabia, M.; Aguilella-Arzo, M.; Angelova, A.; Lesieur, S.; Ricart, S.; Faraudo, J.; Ventosa, N.; Veciana, J. Quatsomes: Vesicles Formed by Self-Assembly of Sterols and Quaternary Ammonium Surfactants. *Langmuir* **2013**, *29*, 6519−6528.
(32) Cui, Z. K.; Bouisse, A.; Cottenye, N.; Lafleur, M. Formation of pH-Sensitive Cationic Liposomes from a Binary Mixture of Monoalkylated Primary Amine and Cholesterol. *Langmuir* **2012**, *28*, 13668−13674.
(33) Cano-Sarabia, M.; Angelova, A.; Ventosa, N.; Lesieur, S.; Veciana, J. Cholesterol Induced CTAB Micelle-to-Vesicle Phase Transitions. *J. Colloid Interface Sci.* **2010**, *350*, 10−15.
(34) Kato, K.; Walde, P.; Koine, N.; Ichikawa, S.; Ishikawa, T.; Nagahama, R.; Ishihara, T.; Tsujii, T.; Shudou, M.; Omokawa, Y.; Kuroiwa, T. Temperature-Sensitive Nonionic Vesicles Prepared from Span 80 (Sorbitan Monooleate). *Langmuir* **2008**, *24*, 10762−10770. Lo, C. T.; Jahn, A.; Locascio, L. E.; Vreeland, W. N. Controlled Self-Assembly of Monodisperse Niosomes by Microfluidic Hydrodynamic Focusing. *Langmuir* **2010**, *26*, 8559−8566.
(35) Pozzi, D.; Caminiti, R.; Marianecci, C.; Carafa, M.; Santucci, E.; De Sanctis, S. C.; Caracciolo, G. Effect of Cholesterol on the Formation and Hydration Behavior of Solid-Supported Niosomal Membranes. *Langmuir* **2010**, *26*, 2268−2273.
(36) Ghosh, S.; Ghatak, C.; Banerjee, C.; Mandal, S.; Kuchlyan, J. Spontaneous Transition of Micelle-Vesicle-Micelle in a mixture of Cationic Surfactant and Anionic Surfactant like Ionic Liquid: A Pure Non-lipid Small Unilamellar Vesicular Template Used for Solvent and Rotational Relaxation Study. *Langmuir* **2013**, *29*, 10066−10076.
(37) Yin, H.; Lei, S.; Zhu, S.; Huang, J.; Ye, J. Micelle-to-Vesicle Transition Induced by Organic Additives in Catanionic Surfactant Systems. *Chem.—Eur. J.* **2006**, *12*, 2825−2835.
(38) Tian, M.; Zhu, L.; Yu, D.; Wang, Y.; Sun, S.; Wang, Y. Aggregate Transitions in Mixtures of Anionic Sulfonate Gemini Surfactant with Cationic Ammonium Single-Chain Surfactant. *J. Phys. Chem. B* **2013**, *117*, 433−440.
(39) Shioi, A.; Hatton, T. A. Model for Formation and Growth of Vesicles in Mixed Anionic/Cationic (SOS/CTAB) Surfactant Systems. *Langmuir* **2002**, *18*, 7341−7348.
(40) Hao, J.; Liu, W.; Xu, G.; Zheng, L. Vesicles from Salt-Free Cationic and Anionic Surfactant Solutions. *Langmuir* **2003**, *19*, 10635−10640.
(41) Makayssi, A.; Bury, R.; Treiner, C. Thermodynamics of Micellar Solubilization for 1-Pentanol in Weakly Interacting Binary Cationic Surfactant Mixtures at 25°C. *Langmuir* **1994**, *10*, 1359−1365.
(42) Mondal, J. A.; Nihonyanagi, S.; Yamaguchi, S.; Tahara, T. Structure and Orientation of Water at Charged Lipid Monolayer/Water Interfaces Probed by Heterodyne-Detected Vibrational Sum Frequency Generation Spectroscopy. *J. Am. Chem. Soc.* **2010**, *132*, 10656−10657.
(43) Nandi, N.; Bhattacharyya, K.; Bagchi, B. Dielectric Relaxation and Solvation Dynamics of Water in Complex Chemical and Biological Systems. *Chem. Rev.* **2000**, *100*, 2013−2045.
(44) Nandi, N.; Bagchi, B. Dielectric Relaxation of Biological Water. *J. Phys. Chem. B* **1997**, *101*, 10954−10961.
(45) Bhattacharyya, K. Solvation Dynamics and Proton Transfer in Supramolecular Assemblies. *Acc. Chem. Res.* **2003**, *36*, 95−101.
(46) Pal, S. K.; Zewail, A. H. Dynamics of Water in Biological Recognition. *Chem. Rev.* **2004**, *104*, 2099−2123.
(47) Robinson, G. W., Singh, S. B., Evans, M. W., Eds. *Water in Biology, Chemistry and Physics*; World Scientific: Singapore, 1996; Chapter 7.
(48) Teeter, M. M. Water−Protein Interactions: Theory and Experiment. *Annu. Rev. Biophys. Biophys. Chem.* **1991**, *20*, 577−600.
(49) Mojumdar, S. S.; Ghosh, S.; Mondal, T.; Bhattacharyya, K. Solvation Dynamics under a Microscope: Single Giant Lipid Vesicle. *Langmuir* **2012**, *28*, 10230−10237.

(50) Sasmal, D. K.; Ghosh, S.; Das, A. K.; Bhattacharyya, K. Solvation Dynamics of Biological Water in a Single Live Cell under a Confocal Microscope. *Langmuir* **2013**, *29*, 2289−2298.
(51) Mukherjee, P.; Crank, J. A.; Haldar, M.; Armstrong, D. W.; Petrich, J. W. Assessing the Roles of the Constituents of Ionic Liquids in Dynamic Solvation: Comparison of an Ionic Liquid in Micellar and Bulk Form. *J. Phys. Chem. A* **2006**, *110*, 10725−10730.
(52) Seth, D.; Sarkar, S.; Sarkar, N. Dynamics of Solvent and Rotational Relaxation of Coumarin 153 in a Room Temperature Ionic Liquid, 1-Butyl-3-methylimidazolium Octyl Sulfate, Forming Micellar Structure. *Langmuir* **2008**, *24*, 7085−7091.
(53) Zhang, X.-X.; Liang, M.; Ernsting, N. P.; Maroncelli, M. Conductivity and Solvation Dynamics in Ionic Liquids. *J. Phys. Chem. Lett.* **2013**, *4*, 1205−1210.
(54) Adhikary, R.; Barnes, C. A.; Petrich, J. W. Solvation Dynamics of the Fluorescent Probe PRODAN in Heterogeneous Environments: Contributions from the Locally Excited and Charge-Transferred States. *J. Phys. Chem. B* **2009**, *113*, 11999−12004.
(55) Ghatak, C.; Rao, V. G.; Ghosh, S.; Mandal, S.; Sarkar, N. Solvation Dynamics and Rotational Relaxation Study Inside Niosome, a Nonionic Innocuous Poly(ethylene glycol)-Based Surfactant Assembly: An Excitation Wavelength Dependent Experiment. *J. Phys. Chem. B* **2011**, *115*, 12514−12520.
(56) Jurkiewicz, P.; Olzyńska, A. O.; Langner, M.; Hof, M. Headgroup Hydration and Mobility of DOTAP/DOPC Bilayers: A Fluorescence Solvent Relaxation Study. *Langmuir* **2006**, *22*, 8741−8749.
(57) Maroncelli, M.; Fleming, G. R. Picosecond Solvation Dynamics of Coumarin 153: The Importance of Molecular Aspects of Solvation. *J. Chem. Phys.* **1987**, *86*, 6221−6239.
(58) Villeneuve, M.; Ootsu, R.; Ishiwata, M.; Nakahara, H. Research on the Vesicle-Micelle Transition by ^{1}H NMR Relaxation Measurement. *J. Phys. Chem. B* **2006**, *110*, 17830−17839.
(59) Mandal, U.; Ghosh, S.; Das, D. K.; Adhikari, A.; Dey, S.; Bhattacharyya, K. Ultrafast Fluorescence Resonance Energy Transfer in a Bile Salt Aggregate: Excitation Wavelength Dependence. *J. Chem. Sci.* **2008**, *120*, 15−18.
(60) Roy, D.; Mondal, S. K.; Sahu, K.; Ghosh, S.; Sen, P.; Bhattacharyya, K. Temperature Dependence of Anisotropy Decay and Solvation Dynamics of Coumarin 153 in γ-Cyclodextrin Aggregates. *J. Phys. Chem. A* **2005**, *109*, 7359−7364.
(61) Shirota, H.; Tamoto, Y.; Segawa, H. Dynamic Fluorescence Probing of the Microenvironment of Sodium Dodecyl Sulfate Micelle Solutions: Surfactant Concentration Dependence and Solvent Isotope Effect. *J. Phys. Chem. A* **2004**, *108*, 3244−3252.